JOURNAL OF AGRICULTURAL AND FOOD CHEMISTRY

Penta-*O*-galloyl-*β*-D-glucose Suppresses Prostate Cancer Bone Metastasis by Transcriptionally Repressing EGF-Induced MMP-9 Expression

PO-TSUN KUO,[†] TSUNG-PANG LIN,[‡] LIANG-CHIH LIU,[†,§] CHI-HUNG HUANG,[†] JEN-KUN LIN,[‡] JUNG-YIE KAO,*[,†] AND TZONG-DER WAY*[,||]

Institute of Biochemistry, College of Life Science, National Chung Hsing University, Taichung, Taiwan, Institute of Biochemistry and Molecular Biology, College of Medicine, National Taiwan University, Taipei, Taiwan, Department of Surgery, Fong-Yuan Hospital Department of Health Executive Yuan, Taichung, Taiwan, and School of Biological Science and Technology, College of Life Science, China Medical University, Taichung, Taiwan

Prostate carcinoma is the most frequently diagnosed malignancy and the second leading cause of cancer-related death of men in the United States. Epidermal growth factor (EGF) generated from bone tissue contributes to prostate cancer metastasis through stimulating matrix metalloproteinase (MMP) secretions from prostate cancer cells. In this study, in vitro invasion assay was performed by incubating penta-*O*-galloyl-*β*-D-glucose (5GG) at various concentrations with 2×10^4 PC-3 cells for 48 h. The anti-invasive and cytotoxic effects of 5GG were found and evaluated on the human androgen-independent prostate cancer PC-3 cell line by MTT assays and Western blot analyses. 5GG inhibited the EGF-induced cell invasiveness and MMP-9 expression in a dose- and time-dependent manner by reducing the MMP-9 transcriptional activity. To explore the mechanisms for the 5GG-mediated regulation of MMP-9, we further examined the effects of 5GG on transcription factors, including NF-κB, AP-1, and mitogen-activated protein kinase (MAPK) activities. The results showed that 5GG suppressed the EGF-induced NF-κB nuclear translocation and also abrogated the EGF-induced activation of c-jun N-terminal kinase (JNK), an upstream modulator of NF-κB. Moreover, we showed that 5GG reduced EGFR expression through the proteasome pathway. These results suggest that 5GG may exert at least part of its anti-invasive effect in androgen-independent prostate cancer by controlling MMP-9 expression through the suppression of the EGFR/JNK pathway. Finally, 5GG suppresses invasion and tumorigenesis in nude mice treatment with intratibia injection of PC-3 cells. These in vitro and in vivo results suggest that 5GG may be a therapeutic candidate for the treatment of advanced prostate cancer.

KEYWORDS: 5GG; MMP-9; EGFR; JNK; invasion; prostate cancer

INTRODUCTION

Prostate cancer is the second leading cause of cancer-related death among men in America (*1*). Although most prostate cancer initially remained sensitive to androgen for therapeutic treatment, many patients eventually relapsed with an androgen resistant disease (*2*). Thus, the prostate carcinoma developed further to an androgen-independent status and became more malignant, metastatic and incurable.

The MMPs, a family of zinc-dependent proteases that degrade the structural components of extracellular matrix, have been shown to engage in tumor invasion. MMPs also play roles in normal bone remodeling and invasion, metastasis and osteolysis of prostate cancer. Inhibition of MMP activity prevents mineralized bone breakdown induced by the addition of PC-3 prostate cancer cells in an in vitro culture system. Particularly, MMP-9 has been found to be specifically associated with prostate cancer metastasis (*3*). High levels of MMP-9 in urine and plasma have been correlated with prostate metastasis (*4*), and inhibition of MMP-9 expression reduced the metastatic potential of prostate cancer cells in mice (*5*).

Bone damage or tumor cells that proliferate in bone tissue induce inflammatory changes (*6*). Inflammation in bone tissue

* Corresponding authors. T.-D.W: School of Biological Science and Technology, College of Life Science, China Medical University, No. 91 Hsueh-Shih Road, Taichung, Taiwan 40402, R.O.C. Tel: (886)-4-2205-3366, ext 2509. Fax: (886)-4-2207-0465. E-mail: tdway@mail.cmu.edu.tw. J.-Y.K.: Institute of Biochemistry, College of Life Science, National Chung Hsing University, Taichung, Taiwan. Tel: (886)-4-22840468, ext 222. Fax: (886)-4-2285-3487. E-mail: jykao@dragon.nchu.edu.tw.

[†] National Chung Hsing University.

[‡] National Taiwan University.

[§] Fong-Yuan Hospital Department of Health Executive Yuan.

[||] China Medical University.

10.1021/jf803725h CCC: $40.75
Published on Web 03/25/2009

is associated with the expression of transforming growth factor-β, which in turn induces the expression of EGF (*7*) in osteoblasts and osteoclasts. EGF is one of the many growth factors that sustain proliferation in a hostile bony microenvironment for metastatic prostate cancer cells and an osteolytic mediator that stimulates prostate cancer cells to produce bone-degrading enzymes, such as parathyroid hormone-related protein (PTHrP) and MMPs (*8*), making bone metastatic prostate cancer cells "osteoclast-like". Indeed, for prostate cancer cells to survive in an undesirable environment as bone tissue, one of the best ways is to become one of them. This is called the osteomimetic property of bone metastatic prostate cancer (*9*).

It has been proposed that stimulation of bone matrix turnover by metastatic prostate cancer cells may be responsible for the tendency of prostate cancer cells to prosper within the bone tissue. This is supposed to trigger a vicious cycle whereby tumor cells stimulate bone metabolism and the substances released during bone matrix turnover enhance the growth of cancer cells that have invaded bone (*3*). EGF and MMPs are important mediators in the communication between tumor cells and bone cells. EGF not only stimulates tumor cell proliferation but also influences osteoclast and osteoblast differentiation (*9*, *10*) whereas inhibition of MMP activity abolishes the mutually supportive cycle between metastatic tumor growth and bone matrix turnover (*3*).

5GG, which is widely dispersed in many medicinal plants, contains one glucose skeleton at which five hydroxyl groups of the glucose are esterified with five gallic acids, respectively. 5GG is widespread and can be found in many medicinal plants. These include the genuses *Rhus*, *Schinus*, *Galla*, *Paeoniae Radix* (the root of *Paeonia lactiflora Pallas*), *Moutan cortex* (the root cortex of *Paeonia suffruicos*), *Macaranga tanariu*, *Quercus pedunculata*, peony, and green alga *Spirogyra varians*. 5GG has been shown to cause several biological activities: it inhibits lipopolysaccharide-induced tumor necrosis factor-α secretion, NADH dehydrogenase I/II, gastric H^+,K^+-ATPase, xanthine oxidase, and α-glucosidase (*11*). 5GG also suppresses tumor growth via inhibition of angiogenesis (*12*) and STAT3 activity in prostate cancer cells (*13*). In our previous studies, we demonstrated that 5GG can induce cell cycle arrest at the G1 phase and apoptosis, and can inhibit proteasome activity and fatty acid synthase expression, suppress lipopolysaccharide-induced activation of NF-κB, and inhibit mouse melanoma cell invasion by suppressing MMP-9 expression (*14*).

Because EGF generated from bone tissue contributes to prostate cancer metastasis through stimulating secretion of MMPs from prostate cancer cells, blocking the interaction between prostate cancer and osteoclast may help to reduce cancer-associated osteolysis and prostate cancer bone metastasis. For this reason, we analyzed the induction of MMPs by EGF in human prostate cancer PC-3 cells and intended to find out the possible mechanism by which 5GG inhibits EGF-induced MMPs secretion from PC-3 cells.

MATERIALS AND METHODS

Cell Cultures and Drug Treatments. The human prostate cancer cell line PC-3 was obtained from The American type Culture Collection (Rockville, MD) and propagated in 100 mm culture dishes at the desired density in RPMI-1640 medium supplemented with 10% fetal calf serum (FCS) (Gibco, Grand Island, NY) in a 5% CO_2 atmosphere at 37 °C. Mouse fibroblast 3T3-L1 was maintained in Dulbecco's modified Eagle medium (DMEM) supplemented with 10% fetal calf serum and incubated in the same condition as that of PC-3 cells. For experiments, PC-3 cells were starved in serum-free medium for 24 h, pretreated with designated drugs for 1 h before EGF stimulation.

Materials and Antibodies. 5GG was isolated from the leaves of *Macaranga tanarins* (L.) as described previously (*15*). EGF, LY294002, PD98059, SB203580, JNK inhibitor II, MG132 (carbobenzoxy-L-leucyl-L-leucyl-L-leucinal) and chloroquine were obtained from Sigma (St. Louis, MO). Anti-MMP-9 antibody was from Chemicon (Temecula, CA). Antihuman PARP antibody was from Phar Mingen (San Diego, CA). Anti-Hsp90 antibody was from Transduction Laboratory (Lexington, KY). Anti-ERK1/2 antibody was from Upstate Biotechnology, Inc. (Lake Placid, NY). Anti-c-jun and c-fos antibodies were from Oncogene (Boston, MA). Antibodies against p-Akt (Ser473), Akt, p-p38, p38 and p-JNK1/2 were from Cell Signaling (Beverly, MA). Antibodies for actin, NF-κB, I-κBα, p-I-κBα, p-ERK1/2, JNK1/2, p-EGFR and EGFR were purchased from Santa Cruz Biotechnology (Santa Cruz, CA). The reagents used in our experiments were prepared in 100 mM stock except for EGF, which was prepared in 50 ng/μL, and antibodies were diluted according to the experimental situation.

MTT Assay. Cells were seeded in a 24-well microtiter plate (2×10^4 cells/well) overnight, then treated with 5GG at various concentrations, and incubated at 24, 48 and 72 h intervals. The effect of 5GG on cell growth was examined by the MTT (3-(4,5-dimethylthiazol-2-yl)-2,5-diphenyl tetrazolium bromide) assay. Briefly, 40 μL of MTT solution (2 mg/mL, Sigma Chemical Co.) was added to each well to make a final volume of 500 μL and incubated for 1 h at 37 °C. The supernatant was aspirated, and the MTT-formazan crystals formed by metabolically viable cells were dissolved in 200 μL of DMSO. Finally, the absorbance of OD at 550 nm was detected and recorded with enzyme-linked immunosorbent assay (ELISA) reader.

In Vitro Invasion Assay. The invasive ability of the cells was assayed in Transwell chambers (Costar, Cambridge, MA) with 8 μm pore size polycarbonate membrane, according to the manufacturer's instructions. Briefly, 2×10^4 cells were seeded in the upper well of each chamber precoated with 30 μg/well reconstituted basement membrane Matrigel (Collaborative Biomedical Products, Bedford, MA), and 3T3-L1 mouse fibroblast conditioned medium was placed in the lower compartment. After incubation, cells were fixed with 10% formaldehyde and stained with Comassie Brilliant Blue. Cells in the upper chamber were removed with a cotton swab. The invasive cells were photographed under a microscope.

Preparation of Nuclear and Cytosolic Fractions. The cells (6×10^5) were cultured on a 100 mm culture dish in 10% FCS RPMI-1640 for 24 h. These cells were then incubated in serum-free RPMI-1640 for another 24 h to avoid the effect of growth factors in serum and then pretreated with 5GG for 1 h, followed by EGF stimulation with designated times. Cells were washed twice with cold PBS and then scraped to an eppendorf in 1 mL of PBS, centrifuged at 4 °C, 12,000 rpm for 5 min. Discarding the supernatant, the pellet was homogenized in 30 μL of hypotonic lysis buffer (HEPES (pH 7.6) 10 mM, EDTA 0.1 mM, dithiothreitol (DTT) 1 mM, PMSF 0.5 mM) by gentle pipetting. After repeated homogenization, the homogenate was centrifuged at 4 °C, 12,000 rpm for 10 min. The supernatant was the cytosolic fraction and was kept at −70 °C overnight. The pellet was washed twice in 20 μL of hypotonic lysis buffer to remove residual cytosolic proteins. After washing, the pellet was dissolved in 30 μL of hypertonic lysis buffer (HEPES (pH 7.6) 20 mM, EDTA 1 mM, DTT 1 mM PMSF 0.5 mM, 25% glycerol, 0.4 M NaCl), pipetted to homogeneity, fiercely vortexed, and then stored at −70 °C overnight. Next day, the solution was centrifuged to collect the supernatant, which was the nuclear fraction. The cytosolic and nuclear fractions were quantified, and equal amounts of protein were subjected to Western blotting.

Western Blot Analysis. The serum-starved cells were pretreated with 5GG for 1 h and then stimulated with EGF for designated times. Afterward, cells were harvested, washed twice with cold PBS, and then lysed in gold lysis buffer (10% glycerol, 1% Triton X-100, 137 mM NaCl, 10 mM NaF, 1 mM EGTA, 5 mM EDTA, 1 mM sodium pyrophosphate, 20 mM Tris-HCl, pH 7.9, 100 mM β-glycerophosphate, 1 mM sodium orthovanadate, 0.1% SDS, 10 μg/mL aprotinin, 1 mM phenylmethylsulfonyl fluoride, and 10 μg/mL leupeptin). Protein concentration was determined by the Bio-Rad protein assay kit (Bio-Rad Laboratories) according to the manufacturer's instructions. A total of 50 μg of protein was separated by SDS−PAGE and transferred to the PVDF membrane (Schleicher & Schuell, Inc., Keene, NH).

Nonspecific binding on the PVDF membrane was minimized with a blocking buffer containing 20 mM Tris-HCl pH 7.4, 125 mM NaCl, 1% BSA and 0.2% sodium azide. Then the membrane was incubated with primary antibodies followed by incubation with horseradish peroxidase-conjugated secondary antibody (Roche Applied Science, Indianapolis, IN). Reactive bands were visualized using an enhanced chemiluminescence system (Amersham Biosciences, Arlington Heights, IL).

Reverse Transcription PCR. Total RNA was extracted from cancer cells using a TRIzol kit (MDBio, Rockville, MD). The reverse transcription reaction was performed using 2 μg of total RNA that was reversely transcribed into cDNA using oligo(dT) primer, then amplified for 30 cycles using two ODN primers: MMP-2 sense GTGCTGAAGGACACACTAAAGAAGA and antisense TTGCCATCCTTCTCAAAGTTGTAGC; MMP-9 sense CACTGTCCACCCCTCAGAGC and antisense GCCACTTGTCGGCGATAAGC; MMP-13 sense TGCTCGCATTCTCCTTCAGGA and antisense ATGCATCCAGGGGTCCTGGC; glyceraldehyde-3-phosphate dehydrogenase sense ACCACAGTCCATGCCATCAC and antisense TCCACCACCCTGTTGCTGTA. Each PCR cycle was carried out for 30 s at 94 °C, 30 s at 55 °C and 1 min at 68 °C. PCR products were separated by 2% agarose DNA electrophoresis gel.

Tranfection. One day before transfection, 2×10^5 cells without serum and antibiotics were plated in six-well plates. Starved PC-3 cells were grown to 90% confluent and transfeted on following day by Lipofectamine 2000 (Invitrogene, Carlsbad, CA), premixed plasmid DNA with OPTI-MEM (GIBCO) for 5 min and than added to each well. After 24 h of incubation, the transfection was completed.

Intratibia Injection of PC-3 in Nude Mice. PC-3 cells were cultured with fresh culture medium for 24 h before intratibia injection. Cancer cells were harvested with trypsin-EDTA (Invitrogen, Carlsbad, CA) and suspended in PBS. The cancer cells were kept at 4 °C before intratibia injection. Intratibia injection of cancer cells was performed using a 30 gauge needle with a polyethylene tube (Recorder No. 427401, Becton Dickinson) fit around the needle. This design is used for making sure of the depth (1.5 mm) of needle inserted into the proximal tibia, preventing the cell suspension from spilling the injection site. Cell suspension (0.3 mL) containing 1×10^6 cells were slowly injected into the bone marrow cavity of tibia. A tumor mass was visualized around the proximal tibia, randomized and divided into 2 groups. The control group was treated with DMSO, and the treated groups were treated ip with 5GG (25 mg/kg) three times a week. For making sure of bone osteolysis, radiographs were taken by a soft X-ray generating unit (Young-kid Enterprise Co., Ltd., Taipei, Taiwan). Animals were deeply anesthetized with trichloroacetaldehyde monohydrate, laid down in a prone position on a Kodak Scientific Imaging film (13 × 18 cm), and X-ray exposure was performed at 45 kV for 5 s.

Statistics. Values are given as mean ± SEM. The significance of difference between the experimental groups and the control groups was assessed by Student's *t* test. The difference is significant if the *P* value is <0.05.

RESULTS

5GG Inhibited Androgen-Independent Prostate Cancer Cells PC-3 Invasion. To determine whether 5GG could affect EGF-induced invasion of PC-3 cells, in vitro invasion assay was performed by incubating 5GG at various concentrations with 2×10^4 PC-3 cells for 48 h. We observed the dose-dependent reduction of invasive cells at a minimum of 5 μM of 5GG treatment (**Figure 1A**,**B**). Ten μM of 5GG reduced the invasive cells more effectively. 20 and 40 μM 5GG treatment almost abolished the invasion of PC-3 cells completely. However, we could not ignore the fact that the cell viability might be affected by the high-dose treatment of 5GG. In order to examine the cytotoxicity of 5GG treatment, we performed MTT assay as follows.

Low Cytotoxicity of 5GG on PC-3 Prostate Cancer Cells. PC-3 cells were treated with various concentrations of 5GG for 24 h, 48 and 72 h. At the end of treatment, cells were harvested and subjected to MTT assay to determine the cell viability. As shown in **Figure 1C**, only long-term exposure of 5GG could cause a cytotoxic effect on PC-3 cells. Although 24 and 48 h treatment of 5GG showed less growth-inhibitory effects on PC-3 cell viability, the inhibition curves were slowed down at 20−70 μM of 5GG treatment, suggesting that 5GG did not exert much toxicity to PC-3 cells between 0 and 48 h, unless over 72 h of treatment. In order to rule out the cytotoxic effect of high concentration treatment, 10 μM 5GG was applied for the following experiments.

Inhibition of 5GG on EGF-Induced MMP-9 Expression in PC-3 Cells. In our previous study, we showed that 5GG can inhibit MMP-9 expression in a mouse melanoma cell line (*14*). In this study, to investigate whether the invasion-inhibitory effect of 5GG resulted from the suppression of MMP-9 induction by EGF, we analyzed EGF-induced MMP-9 expression in 5GG-treated PC-3 cells by Western blotting. **Figure 2A** showed that 5GG inhibited EGF-induced MMP-9 expression in a dose-dependent manner. As shown in **Figure 2B**, 5GG exerted its inhibitory effect on EGF-induced MMP-9 expression via a time-dependent manner when cells were incubated with 10 μM of 5GG.

Suppression of MMP-9 mRNA Expression by 5GG. In order to investigate whether the suppression of MMP-9 protein by 5GG was due to reduced MMP-9 mRNA expression, RT-PCR analysis was employed on total mRNA samples extracted from PC-3 cells after EGF treatment. The amplification of cDNA with primers specific for MMP-9 and G3PDH (as control gene) was shown in **Figure 2C**. 5GG repressed the expression of MMP-9 mRNA in a dose-dependent manner. We also looked over the mRNA expression of MMPs (MMP-2, MMP-13) family that involved in metastasis. As shown in **Figure 2D**, 5GG did not repress the expression of MMP-2 and MMP-13 mRNA. The data suggest that 5GG modulated MMP-9 expression at the transcriptional level.

Down-Regulation of EGF-Induced NF-κB Nuclear Translocation by 5GG. Transcription factors NF-κB and AP-1 have been reported to control MMP-9 gene expression (*16*). Thus, we examined the localization of NF-κB and AP-1 in nuclear and cytosolic fractions from PC-3 cells to determine whether these transcription factors were involved in regulating MMP-9 gene expression. As shown in **Figure 3**, we found that EGF induced NF-κB nuclear translocation from cytosol in a time-dependent manner while pretreatment of 5GG down-regulated EGF-mediated NF-κB nuclear translocation. Cytosolic I-κBα reduced as the induction time increased and 5GG pretreatment prevented EGF-induced I-κBα degradation. Moreover, phospho-I-κBα was increased upon EGF stimulation. 5GG pretreatment decreased phospho-I-κBα, making I-κBα unfavorable for degradation. Nuclear I-κBα and phospho-I-κBα were also blotted to make sure that there was minimal contamination.

The action of AP-1, composed of c-jun and c-fos, was quite different from that of NF-κB because it accumulated maximally in the nuclear fraction as fast as 30 min induction and gradually decreased while NF-κB slowly translocated into the nuclear fraction and reached its maximum amount as late as 120 min. To our surprise, 5GG pretreatment potentiated c-jun and c-fos nuclear translocation, suggesting that NF-κB nuclear translocation rather than AP-1 nuclear translocation was the major prerequisite to up-regulate EGF-induced MMP-9 expression. PARP and Hsp90 served as nuclear and cytosolic internal controls, respectively. Taken together, these findings clearly indicated that 5GG inhibited EGF-induced NF-κB nuclear translocation.

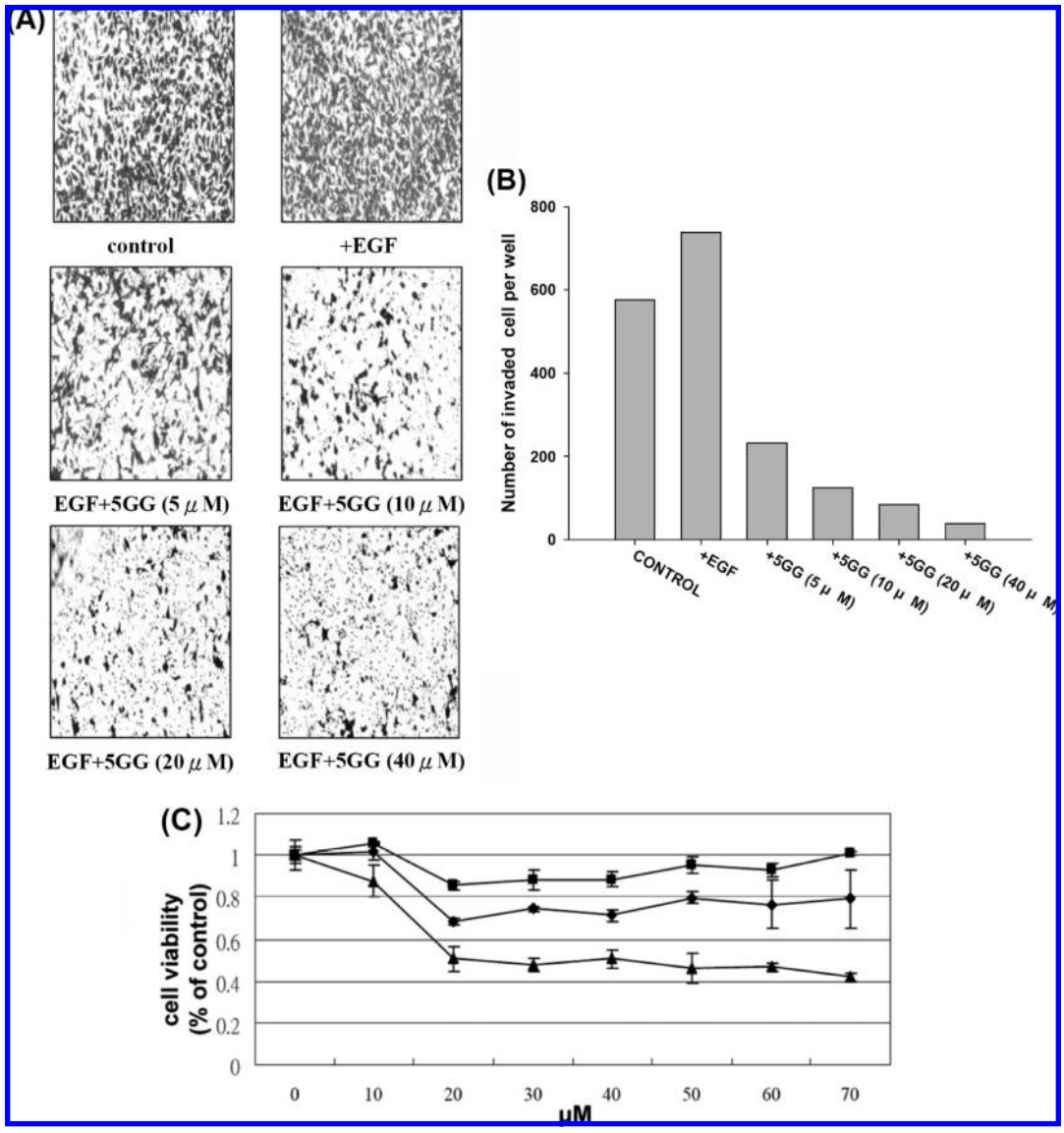

Figure 1. Effect of 5GG on EGF-induced invasion of PC-3 cells. (**A**) Various concentrations of 5GG pretreatments were followed by EGF (25 ng/mL) stimulation for 48 h. In vitro invasion assay was performed according to the manufacturer's instructions and photographed under a microscope (Leica DMIRB) at 100×. (**B**) The number of migrations through Materigel matrix cells was quantified by counting in each well. (**C**) MTT assay of 5GG on PC-3 prostate cancer cells. Twenty-four hours (■), 48 h (◆) and 72 h (▲) accompanied with various concentrations of 5GG treatments were tested, and cell viability was expressed as the percentage of the control (defined as 100%). Shown are means ± SE for three separate experiments.

Inhibition of 5GG on EGF-Induced JNK2 Phosphorylation. It is still unclear that which signal transduction pathways elicited by EGF are responsible for regulating NF-κB localization. To find out the possible upstream pathways contributing to NF-κB nuclear translocation by EGF stimulation, we investigated four kinase candidates that might control NF-κB nuclear translocation in response to EGF stimulation (*17*, *18*). Akt, ERK1/2, p38 and JNK1/2 were chosen, and their phosphorylation statuses were determined by Western blotting using specific antiphospho-form antibodies. Because it is well-known that the stimulatory effect of EGF is aroused within a short time, we detected the activation statuses of the four pathways within an hour. As shown in **Figure 4A**, we found that Akt was rapidly activated by EGF at 5min and gradually returned to its unstimulated status, but 5GG prolonged the activation of Akt for 30 min, suggesting that the Akt pathway may not be a possible candidate in regulating NF-κB nuclear translocation under EGF stimulation because it was not inhibited by 5GG treatment. EGF also activated ERK1/2 and phosphorylated ERK1/2 went back to its unstimulated status as early as 15 min. The effect of 5GG on ERK1/2 phosphorylation coincided with the untreated one, suggesting that 5GG did not affect EGF-induced ERK1/2 signaling. EGF stimulation seemed to slightly activate p38, and 5GG pretreatment did not make much difference on the pattern of the bands with the untreated ones. JNK1/2 was activated and its phosphorylation lasted for an hour by EGF stimulation; in contrast, 5GG pretreatment inhibited JNK1/2 phosphorylation by EGF, especially at JNK2, which was correlated with the down-regulation of NF-κB nuclear translocation by 5GG pretreatment (**Figure 4A**).This raised the possibility that 5GG inhibits EGF-induced NF-κB nuclear translocation by suppression of JNK1/2 activation. In order to further confirm the inhibitory effect of 5GG on EGF-induced JNK1/2 phosphorylation, we elongated the times tested (**Figure 4B**). As expected, the phosphorylation of JNK1/2, especially JNK2, was inhibited even at 12 h, further confirming that 5GG inhibited EGF induced JNK phosphorylation.

Inhibition of 5GG on EGF-Induced EGFR Phosphorylation and EGFR Expression. The inhibition of 5GG on EGF-induced JNK phosphorylation made us ask whether 5GG exerts

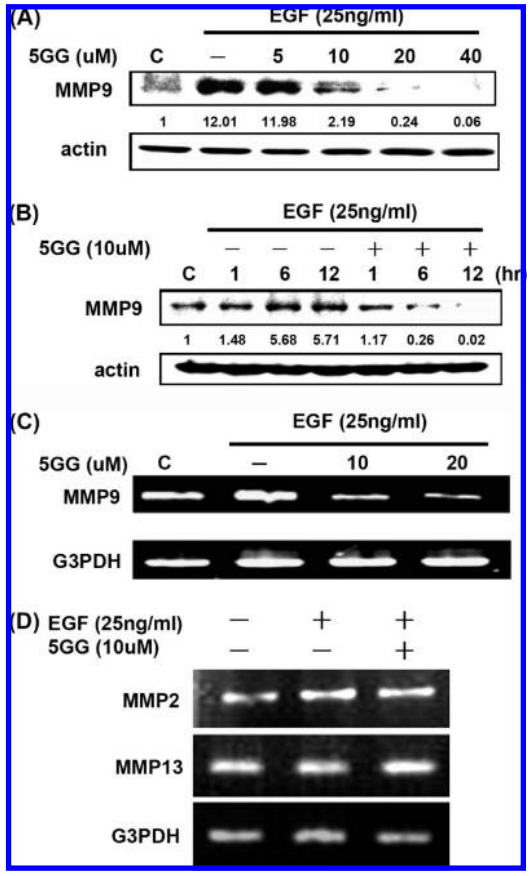

Figure 2. EGF-induced MMP-9 expression was decreased by 5GG treatment. PC-3 cells were serum-starved for 24 h followed by 5GG pretreatment for 1 h and EGF stimulation. Dose (**A**) and time course (**B**) experiments are shown. Immunoblotting was used to measure levels of MMP-9 and actin. Western blot data presented are representative of those obtained in at least three separate experiments. The values below the figures represent change in protein expression of the bands normalized to actin. PC-3 cells were pretreated with/without 5GG for 1 h followed by EGF stimulation for 6 h, and mRNA of MMP-9 (**C**), MMP-2, MMP-13 (**D**) and G3PDH mRNA were determined. RT-PCR data presented are representative of those obtained in at least three separate experiments.

its inhibitory effect on a more upstream element, and whether the inhibition of these downstream elements was due to inhibition of the upper stream elements. Thus, we examined the effect of 5GG on the most upstream element, in this system, EGFR. As shown in **Figure 5A**, EGF induced EGFR phosphorylation and EGFR down-regulation, consistent with the well-known phenomena in EGF-EGFR interaction (*19*). However, 5GG pretreatment before EGF stimulation not only inhibited EGFR phosphorylation but also strongly decreased the EGFR protein level. To further confirm these findings, the extended periods of time were tested and the results are shown in **Figure 5B**. Indeed, 5GG did both inhibit EGF-induced EGFR phosphorylation and reduce EGFR protein level strongly, compared to the untreated ones. This finding was inspiring because we found that EGFR, which is a good therapeutic target in many cancer-related diseases, was inhibited by 5GG treatment.

Proteasome Was Involved in 5GG-Mediated EGFR Down-Regulation. 5GG-induced phospho-EGFR down-regulation under EGF stimulation was accompanied by a decrease of the EGFR protein level. It seems that 5GG lowered phospho-EGFR due to the reduction of EGFR protein. Since EGFR protein expression was decreased rapidly within an hour, we suggest that 5GG influenced the stability of EGFR protein, but not the transcription or translation of EGFR. In order to confirm this hypothesis, we searched the reports that described EGFR turnover. It was accepted that both proteasome and lysosome were involved in EGFR degradation (*19*). Therefore, we applied the proteasome inhibitor MG132 and the lysosome inhibitor chloroquine to test if these two inhibitors can rescue 5GG-mediated EGFR degradation. As shown in **Figure 6A**, we showed that 5GG induced EGFR down-regulation with or without EGF stimulation. Pretreatment of MG132 restored EGFR expression and phosphorylation, suggesting that proteasome was involved in 5GG-mediated EGFR down-regulation and the recovery of phospho-EGFR was due to restored EGFR expression. Recovered EGFR expression and EGFR phosphorylation were accompanied by restored JNK1/2 phsphorylation, indicating the related association between EGFR and JNK1/2.

Involvement of EGFR and JNK1/2 in 5GG-Mediated MMP-9 Down-Regulation. To further confirm the link among EGFR/JNK/MMP-9, we used MG132 to test if recovered EGFR expression could lead to recovery of JNK1/2 phosphorylation and MMP-9 expression. We showed that 5GG-induced EGFR, JNK1/2 and MMP-9 down-regulation under EGF stimulation could all be rescued by MG132 (**Figure 6B**), indicating that there was a correlation among these three factors and 5GG-mediated MMP-9 down-regulation may result from the inhibition of EGFR/JNK pathway. Finally, to truly assess which of the four signal pathways elicited by EGF stimulation regulated MMP-9 expression, we applied inhibitors for each signal pathway and examined MMP-9 expression. We found that JNK1/2 inhibitor strongly inhibited EGF-induced MMP-9 expression whereas the other three inhibitors did not have any effects (**Figure 6C**). These results indicate the link among EGFR/JNK/MMP-9 signaling.

Overexpression of EGFR Increased 5GG-Induced MMP-9 Down-Regulation. To further examine the role of EGFR and JNK in 5GG-induced MMP-9 down-regulation, EGFR was transfected into PC-3 cells. Western blotting analysis revealed that 5GG-induced MMP-9 and p-JNK1/2 down-regulation effects were abolished by transfection with EGFR (**Figure 7**). These results demonstrated that MMP-9 expression was involved in EGFR and JNK signal pathway.

5GG Suppresses Invasion and Tumorigenesis in Nude Mice of Intratibia Injection of PC-3 Cells. 5GG is an attractive therapeutic drug, but the efficacy of this approach has yet to be demonstrated in vivo. To examine the effect of 5GG on tumor growth, PC-3 cells were locally injected into the bone marrow cavity of tibia in nude mice (4 weeks old). Mice were randomized and divided into 2 groups. The control group was treated with DMSO, and the treated groups were treated ip with 5GG (25 mg/kg) three times a week. A visible spherical tumor mass appeared in the proximal tibia 28 days later in nude mice. 5GG showed significant antitumor activity (**Figure 8B**). Moreover, body weights were not significantly affected by 5GG. For making sure of bone osteolysis, radiographs were taken by a soft X-ray generating unit. Radiographs taken on day 28 revealed that osteolytic lesions appeared in the control cancer cell-injected tibia. On the other hand, lesion areas markedly declined in the 5GG group (**Figure 8A**). Quantitative assessment of osteolysis and tumor weight indicated that 5GG treatment inhibited both osteolytic lesion and tumor size.

DISCUSSION

Most patients with cancer die not because of the primary tumor growth but rather because of the spread of tumor cells to

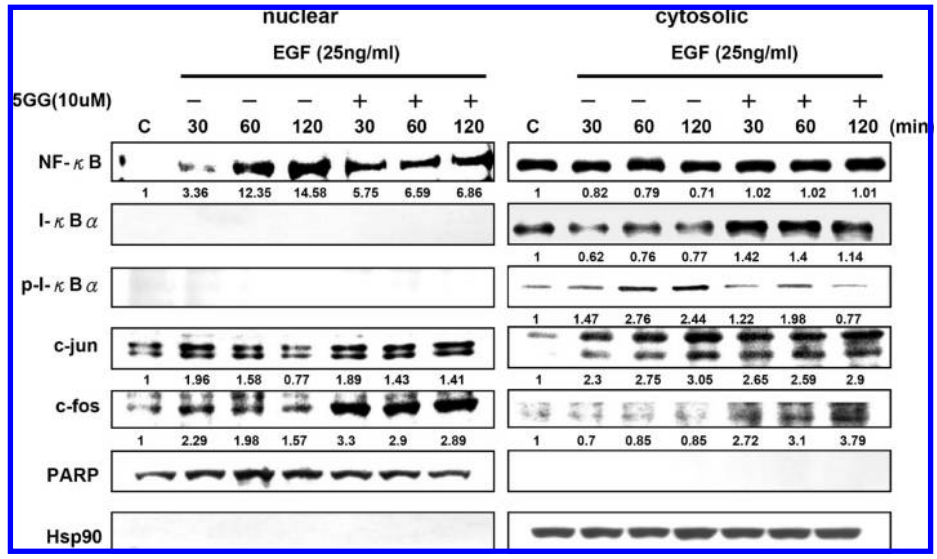

Figure 3. Effect of 5GG on EGF-induced NF-κB and AP-1 nuclear translocation. PC-3 cells were pretreated with/without 5GG for 1 h followed by EGF stimulation for 30, 60 or 120 min. The cell lysates were separated into nuclear and cytosolic fractions. Levels of NF-κB, I-κBα, p-I-κBα, c-jun, c-fos PARP and Hsp90 were analyzed by immunoblotting. PARP and Hsp90 served as nuclear and cytosolic internal controls, respectively. Western blot data presented are representative of those obtained in at least three separate experiments. The values below the figures represent change in protein expression of the bands normalized to control.

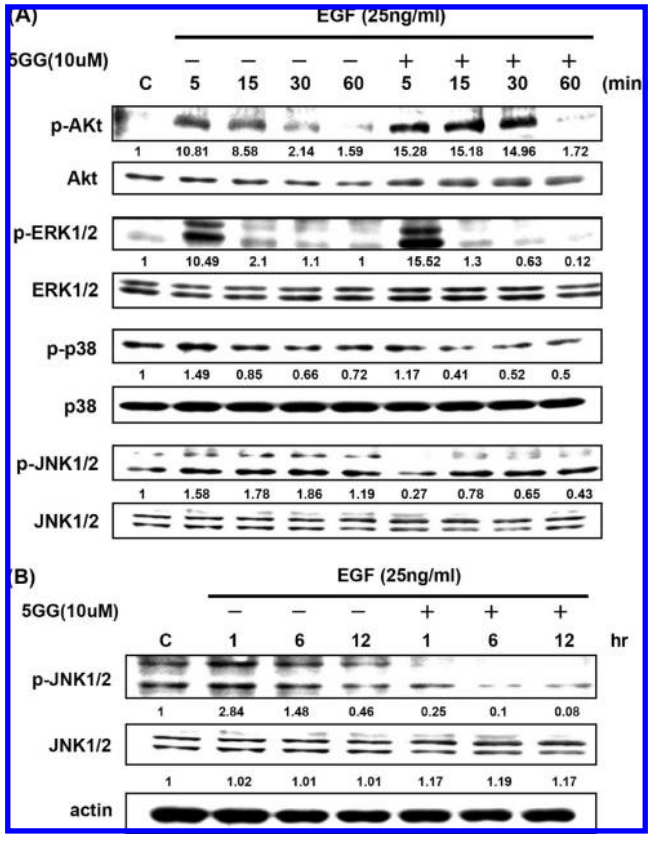

Figure 4. Effect of 5GG on EGF-induced phosphorylation of Akt, JNK1/2, p38 and ERK1/2. (**A**) PC-3 cells were pretreated with/without 5GG for 1 h followed by EGF stimulation for 5, 15, 30 or 60 min. Levels of p-Akt, Akt, p-ERK1/2, ERK1/2, p-p38, p38, p-JNK1/2 and JNK1/2 were analyzed by immunoblotting. (**B**) A prolonged time course experiment at 1, 6 and 12 h intervals was applied to analyze the activation of JNK1/2 by EGF stimulation and inactivation under 5GG treatment. Western blot data presented are representative of those obtained in at least three separate experiments. The values below the figures represent change in protein expression of the bands normalized to control.

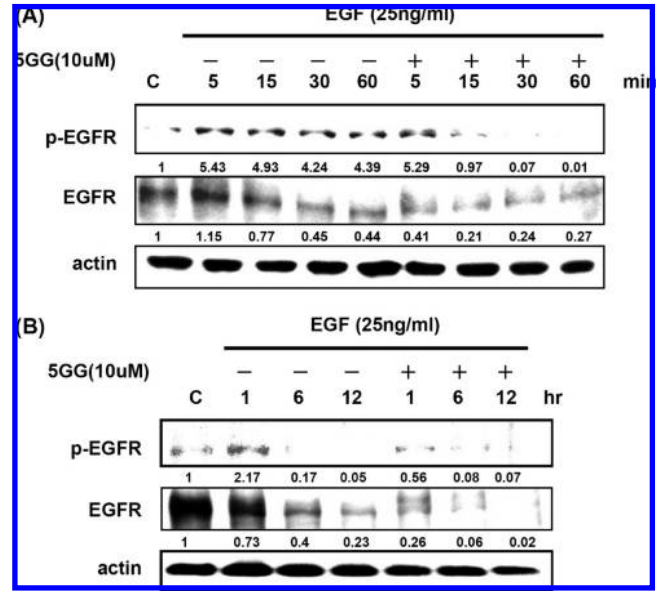

Figure 5. Effect of 5GG on the EGFR protein level and phosphorylation. (**A**) PC-3 cells were pretreated with/without 5GG for 1 h followed by EGF stimulation for 5, 15, 30 or 60 min and analyzed the activation of EGFR by Western blotting. (**B**) A prolonged time course experiment at 1, 6 and 12 h intervals was applied to analyze the activation of EGFR by EGF stimulation and inactivation under 5GG treatment. Western blot data presented are representative of those obtained in at least three separate experiments. The values below the figures represent change in protein expression of the bands normalized to control.

other sites. Patients with advanced prostate cancer almost inevitably develop bone metastases, and the chances are so high that in patients who are originally diagnosed with prostate cancer, the major tumor burdens are in the bone at the time of death (*20*). Prostate cancer bone metastasis causes tremendous morbidity including pain, impaired mobility, pathologic fractures, spinal cord compression and other problems (*3*). It is well accepted that both bone formation and bone breakdown are present within metastatic deposits (*21*), depending on the nature of the metastatic prostate cancer and the interaction between

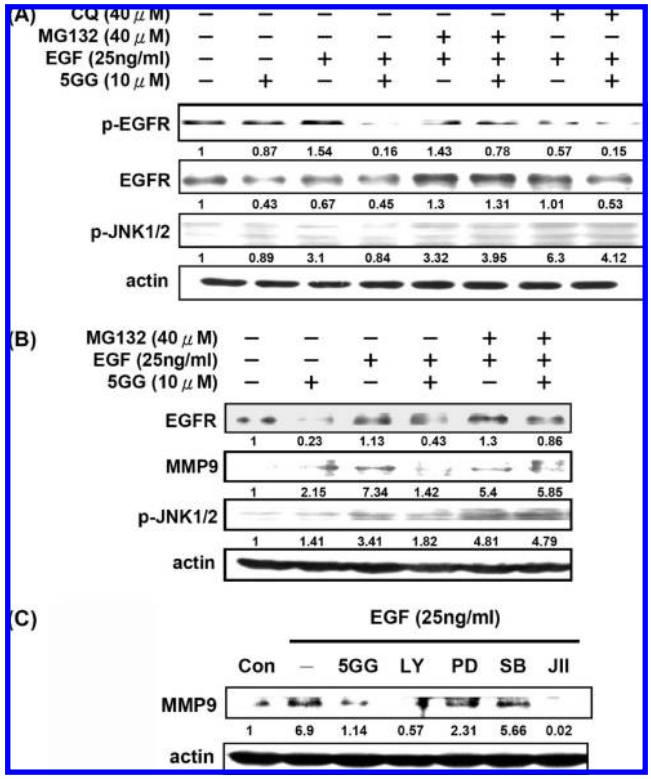

Figure 6. Prevention of proteasome inhibitor on 5GG-mediated EGFR down-regulation under EGF induction and involvement of EGFR and JNK1/2 in 5GG-mediated MMP-9 down-regulation. Proteasome inhibitor MG132 was treated for 1 h before 5GG pretreatment and EGF stimulation. The activation of EGFR and JNK1/2 were analyzed by Western blotting. The induction time of EGF was 1 h (**A**) and 12 h (**B**). (**C**) PC-3 cells were treated with 5GG (10 μM), PI3K inhibitor LY294002 (20 μM), ERK inhibitor PD98059 (16 μM), p38 inhibitor SB203580 (40 μM) or JNK inhibitor JNK Inhibitor II (40 μM) for 1 h followed by EGF induction for 12 h. Western blot data presented are representative of those obtained in at least three separate experiments. The values below the figures represent change in protein expression of the bands normalized to control.

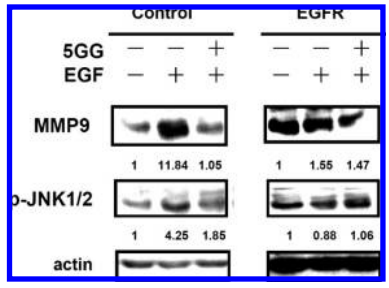

Figure 7. The MMP-9 expression level was reversed by transfected EGFR. EGFR plasmids were transfected into PC-3 cells. After EGFR plasmids were transfected, cells were serum-starved for 24 h followed by 5GG pretreatment for 1 h and EGF stimulation for 6 h. Immunoblotting was used to measure levels of MMP-9 and p-JNK1/2. Western blot data presented are representative of those obtained in at least three separate experiments. The values below the figures represent change in protein expression of the bands normalized to control.

tumor cells and bone microenvironment. However, little is known about the biological mechanisms underlying the stimulation of bone metabolism by metastatic cells.

In previous reports investigating bone metastatic prostate cancer cells, Zellweger et al. (*22*) demonstrated that EGFR expression correlates with the malignancy of prostate cancer, in the development of both AIPC and metastasis. Kim et al. (*6*)

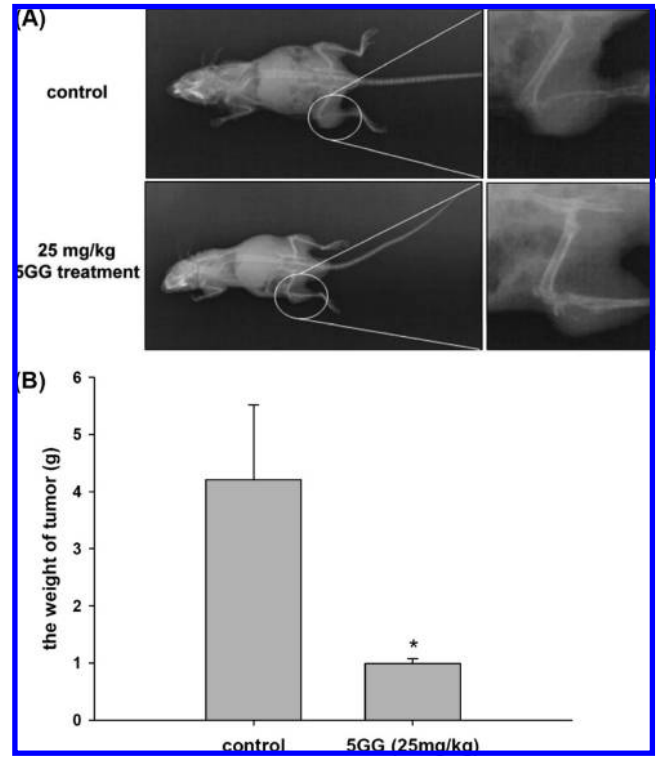

Figure 8. 5GG reduced cancer-associated osteolysis and tumorigenesis. (**A**) We utilized X-ray to observe the osteolysis between treatment with 5GG (25 mg/kg, 3 times per week) and no 5GG treatment as the control. (**B**) The mice with 5GG treatment showed significant tumor weight reduction and statistics by Student's *t* test (* $p < 0.05$).

more specifically showed that the expression of EGFR on the surface of human prostate cancer cells directly correlates with their proximity to bone tissue. Both findings support the significance of EGFR in prostate cancer bone metastasis. Also, chronic EGFR activation can lead to AR down-modulation and functional attenuation under conditions of robust tumor growth in a castrate environment (*23*), suggesting that the EGFR may be able to suppress and consequently bypass AR while supporting conditions that maintain the growth potential of the tumor cells, and finally, the development of AIPC (*24*). The ligand of EGFR, EGF, is also a critical mediator in regulating the proliferation of metastatic prostate cancer cells and the differentiation of osteocytes, establishing the osteomimetic properties of metastatic prostate cancer cells and the vicious cycle between the "seed" and the "soil". Therapeutic targeting of EGFR signaling has been intensely investigated.

The regulation of expression and activity of MMP-9 by EGF has been demonstrated (*25*). MMP activities not only are involved in bone matrix turnover but also stimulate metastatic tumor growth. Thus, the interactions between tumor cells and host cells are interweaved, and redundant pathways may be involved in promoting the malignancy of metastatic cells. Blockade of the communication between tumor cells and host cells may help reduce the mutually supportive cycle and uncover the camouflage of the osteomimetic metastatic prostate cancer cells.

In the present study, we demonstrated that 5GG inhibited EGF-induced MMP-9 expression in a dose- and time-dependent manner, suggesting the potential activity of 5GG in blocking the actions of EGF and MMP-9. We also showed that 5GG inhibited EGF-induced invasion of PC-3 cells in a dose-dependent manner, indicating that the inhibition of MMP-9 expression resulted in the loss of ability for PC-3 cells to degrade

the component of Matrigel and thus the ability to invade in vitro. However, in vivo experiments demonstrating the effect of 5GG on PC-3 cell bone metastasis upon tumor injection on mouse model are still needed.

The signal transduction pathways mediating EGF-induced MMP-9 expression is largely unknown. We took advantage of the inhibitory effect of 5GG on EGF-induced MMP-9 expression to clarify the factors involved in EGF signaling and MMP-9 expression. Since the effect of 5GG was exerted as late as 6 h on MMP-9 protein level, we suggest that the transcriptional regulation of MMP-9 might be inhibited by 5GG. Our RT-PCR data confirmed that 5GG modulated MMP-9 expression at the transcriptional level. We examined transcription factors that have been reported to participate in regulating MMP-9 gene expression (*16*) and found that NF-κB nuclear translocation upon EGF stimulation was inhibited by 5GG while AP-1 resulted contrarily, indicating that NF-κB, rather than AP-1, was the key mediator involved in regulating EGF-induced MMP-9 expression. These findings were in accordance with the previous reports that MMP-9 is NF-κB responsive (*26*) and NF-κB is a pivotal transcription factor in regulating MMP-9 expression in PC-3 cells (*27*). NF-κB has been largely implicated in inflammatory responses and tumor progression, which is also regarded as a kind of inflammation. EGF-induced NF-κB activation mimics inflammatory response and the inhibitory effect of 5GG on NF-κB activation suggests that 5GG may be an anti-inflammation candidate. It is remains unclear why AP-1 nuclear accumulation elicited by 5GG remains unclear. One possibility is due to the stress caused by 5GG; however, the mechanism and biological significance of AP-1 nuclear accumulation requires further investigation.

Subsequently, we explored the possible signal transduction pathways that were involved in mediating EGF signal transduction. Resent studies have demonstrated that three major MAPK subfamilies (ERK 1/2, JNK and p38) and Akt regulate NF-kappaB activation (*17*, *18*). In the present study, we found that 5GG did not affect EGF-induced ERK1/2 and p38 signaling but maintained Akt phosphorylation; however, 5GG dramatically reduced JNK1/2 phosphorylation, especially JNK2. A prolonged time course experiment demonstrated that this inhibitory effect of 5GG lasted as long as 12 h, suggesting the significance of JNK2 in mediating EGF-induced NF-κB activation and MMP-9 expression. Data referring to the role of stress kinase pathways in the activation of NF-κB are limited and controversial. It has been demonstrated that addition of purified MEKK1, activator for the JNK upstream kinase MKK4, to I-κBα kinase complex resulted in the activation of I-κBα kinase (*28*). MEKK1 induction of I-κBα kinase activity is independent of ubiquitination and thus may constitute a separate pathway for NF-κB activation. In our current study, we demonstrated that EGF induced JNK1/2 phosphorylation and the inhibition of 5GG on NF-κB nuclear translocation upon EGF stimulation may result from the inhibition of JNK signaling.

Therapeutic targeting on EGFR has been intensely investigated. Numerous reports document the significance of EGFR in prostate cancer progression (*23*, *25*). In this case, PC-3 cells, androgen-independent and AR-negative, are thought to implicate other oncogenes other than AR signaling to sustain its progression and development of AIPC, for example, EGFR. EGFR is initially involved in embryonic differentiation and rarely expressed in adults. Bone metastatic PC-3 cells may apply this characteristic of EGFR to impel them back to the "stem-cell-like" status, thus rendering these tumor cells having capacity to differentiate in the bone tissue osteomimetically. In addition, strong EGF autocrine and paracrine signalings in PC-3 cells have also been reported (*29*, *30*), further emphasizing the significance of EGFR in prostate cancer progression and metastasis.

Understanding the molecular mechanisms and the signal transduction pathways involved in bone metastatic prostate cancer is a prerequisite for the development of clinical strategies that specifically target prostate cancer bone metastasis. In this study, we demonstrated that 5GG inhibited EGF signaling, including EGFR, JNK1/2, NF-κB and MMP-9 expression, suggesting that 5GG may be a therapeutic candidate for the treatment of advanced prostate cancer.

ABBREVIATIONS USED

5GG, penta-*O*-galloyl-β-D-glucose; MMP-9, matrix metalloproteinase 9; PC-3, prostate cancer cell 3; EGFR, epidermal growth factor receptor; MAPK, mitogen-activated protein kinase; JNK, c-jun N-terminal kinase; G3PDH, glyceraldehyde-3-phosphate dehydrogenase; MTT, 3-(4,5-dimethylthiazol-2-yl)-2,5-diphenyl tetrazolium bromide.

ACKNOWLEDGMENT

The authors wish to thank Mr. William K. Earl for English editing.

LITERATURE CITED

(1) Smith, R. A.; Cokkinides, V.; Brawley, O. W. Cancer screening in the United States, 2009: A review of current American Cancer Society guidelines and issues in cancer screening. *Ca—Cancer J. Clin*. **2009**, *59*, 27–41.

(2) Griffiths, K.; Eaton, C. L.; Harper, M. E.; Turkes, A.; Peeling, W. B. Hormonal treatment of advanced disease: some newer aspects. *Semin. Oncol*. **1994**, *21*, 672–687.

(3) Nemeth, J. A.; Yousif, R.; Herzog, M.; Che, M.; Upadhyay, J.; Shekarriz, B.; Bhagat, S.; Mullins, C.; Fridman, R.; Cher, M. L. Matrix metalloproteinase activity, bone matrix turnover, and tumor cell proliferation in prostate cancer bone metastasis. *J. Natl. Cancer Inst*. **2002**, *94*, 17–25.

(4) Moses, M. A.; Wiederschain, D.; Loughlin, K. R.; Zurakowski, D.; Lamb, C. C.; Freeman, M. R. Increased incidence of matrix metalloproteinases in urine of cancer patients. *Cancer Res*. **1998**, *58*, 1395–1399.

(5) Kong, D.; Li, Y.; Wang, Z.; Banerjee, S.; Sarkar, F. H. Inhibition of angiogenesis and invasion by 3,3′-diindolylmethane is mediated by the nuclear factor-kappaB downstream target genes MMP-9 and uPA that regulated bioavailability of vascular endothelial growth factor in prostate cancer. *Cancer Res*. **2007**, *67*, 3310–3319.

(6) Kim, S. J.; Uehara, H.; Yazici, S.; Langley, R. R.; He, J.; Tsan, R.; Fan, D.; Killion, J. J.; Fidler, I. J. Simultaneous blockade of platelet-derived growth factor-receptor and epidermal growth factor-receptor signaling and systemic administration of paclitaxel as therapy for human prostate cancer metastasis in bone of nude mice. *Cancer Res*. **2004**, *64*, 4201–4208.

(7) Hou, X.; Johnson, A. C.; Rosner, M. R. Induction of epidermal growth factor receptor gene transcription by transforming growth factor beta 1: association with loss of protein binding to a negative regulatory element. *Cell Growth Differ*. **1994**, *5*, 801–809.

(8) Chung, L. W.; Baseman, A.; Assikis, V.; Zhau, H. E. Molecular insights into prostate cancer progression: the missing link of tumor microenvironment. *J. Urol*. **2005**, *173*, 10–20.

(9) Dorai, T.; Dutcher, J. P.; Dempster, D. W.; Wiernik, P. H. Therapeutic potential of curcumin in prostate cancer—V: Interference with the osteomimetic properties of hormone refractory C4-2B prostate cancer cells. *Prostate* **2004**, *60*, 1–17.

(10) Gonzalez, E. A.; Disthabanchong, S.; Kowalewski, R.; Martin, K. J. Mechanisms of the regulation of EGF receptor gene expression by calcitriol and parathyroid hormone in UMR 106-01 cells. *Kidney Int.* **2002**, *61*, 1627–1634.
(11) Fujiki, H. Green tea: Health benefits as cancer preventive for humans. *Chem. Rec.* **2005**, *5*, 119–132.
(12) Huh, J. E.; Lee, E. O.; Kim, M. S.; Kang, K. S.; Kim, C. H.; Cha, B. C.; Surh, Y. J.; Kim, S. H. Penta-O-galloyl-beta-D-glucose suppresses tumor growth via inhibition of angiogenesis and stimulation of apoptosis: roles of cyclooxygenase-2 and mitogen-activated protein kinase pathways. *Carcinogenesis* **2005**, *26*, 1436–1445.
(13) Hu, H.; Lee, H. J.; Jiang, C.; Zhang, J.; Wang, L.; Zhao, Y.; Xiang, Q.; Lee, E. O.; Kim, S. H.; Lü, J. Penta-1,2,3,4,6-O-galloyl-beta-D-glucose induces p53 and inhibits STAT3 in prostate cancer cells in vitro and suppresses prostate xenograft tumor growth in vivo. *Mol. Cancer Ther.* **2008**, *7*, 2681–2691.
(14) Ho, L. L.; Chen, W. J.; Lin-Shiau, S. Y.; Lin, J. K. Penta-O-galloyl-beta-D-glucose inhibits the invasion of mouse melanoma by suppressing metalloproteinase-9 through down-regulation of activator protein-1. *Eur. J. Pharmacol.* **2002**, *453*, 149–158.
(15) Yokozawa, T.; Chung, H. Y.; Oura, H.; Nonaka, G.; Nishioka, I. Isolation of a renal function-facilitating constituent from the Oriental drug, salviae miltiorrhizae radix. *Nippon Jinzo Gakkaishi* **1989**, *31*, 1091–1098.
(16) Westermarck, J.; Kahari, V. M. Regulation of matrix metalloproteinase expression in tumor invasion. *FASEB J.* **1999**, *13*, 781–792.
(17) Uzzo, R. G.; Crispen, P. L.; Golovine, K.; Makhov, P.; Horwitz, E. M.; Kolenko, V. M. Diverse effects of zinc on NF-kappaB and AP-1 transcription factors: implications for prostate cancer progression. *Carcinogenesis* **2006**, *27*, 1980–1990.
(18) Shukla, S.; Maclennan, G. T.; Marengo, S. R.; Resnick, M. I.; Gupta, S. Constitutive activation of P I3 K-Akt and NF-kappaB during prostate cancer progression in autochthonous transgenic mouse model. *Prostate* **2005**, *64*, 224–239.
(19) Alwan, H. A.; van Zoelen, E. J.; van Leeuwen, J. E. Ligand-induced lysosomal epidermal growth factor receptor (EGFR) degradation is preceded by proteasome-dependent EGFR de-ubiquitination. *J. Biol. Chem.* **2003**, *278*, 35781–35790.
(20) Mundy, G. R. Metastasis to bone: causes, consequences and therapeutic opportunities. *Nat. Rev. Cancer* **2002**, *2*, 584–593.
(21) Roato, I.; D'Amelio, P.; Gorassini, E.; Grimaldi, A.; Bonello, L.; Fiori, C.; Delsedime, L.; Tizzani, A.; De Libero, A.; Isaia, G.; Ferracini, R. Osteoclasts are active in bone forming metastases of prostate cancer patients. *PLoS One* **2008**, *3*, e3627.
(22) Zellweger, T.; Ninck, C.; Bloch, M.; Mirlacher, M.; Koivisto, P. A.; Helin, H. J.; Mihatsch, M. J.; Gasser, T. C.; Bubendorf, L. Expression patterns of potential therapeutic targets in prostate cancer. *Int. J. Cancer* **2005**, *113*, 619–628.
(23) Adam, R. M.; Kim, J.; Lin, J.; Orsola, A.; Zhuang, L.; Rice, D. C.; Freeman, M. R. Heparin-binding epidermal growth factor-like growth factor stimulates androgen-independent prostate tumor growth and antagonizes androgen receptor function. *Endocrinology* **2002**, *143*, 4599–4608.
(24) Freeman, M. R. HER2/HER3 heterodimers in prostate cancer: Whither HER1/EGFR? *Cancer Cell* **2004**, *6*, 427–428.
(25) Festuccia, C.; Guerra, F.; D'Ascenzo, S.; Giunciuglio, D.; Albin, i A.; Bologna, M. In vitro regulation of pericellular proteolysis in prostatic tumor cells treated with bombesin. *Int. J. Cancer* **1998**, *75b*, 418–431.
(26) Shukla, S.; Gupta, S. Suppression of constitutive and tumor necrosis factor alpha-induced nuclear factor (NF)-kappaB activation and induction of apoptosis by apigenin in human prostate carcinoma PC-3 cells: correlation with down-regulation of NF-kappaB-responsive genes. *Clin. Cancer Res.* **2004**, *10*, 3169–3178.
(27) Andela, V. B.; Gordon, A. H.; Zotalis, G.; Rosier, R. N.; Goater, J. J.; Lewis, G. D.; Schwarz, E. M.; Puzas, J. E.; O'Keefe, R. J. NFkappaB: a pivotal transcription factor in prostate cancer metastasis to bone. *Clin. Orthop. Relat. Res.* **2003**, *415*, S75–S85, Suppl.
(28) Lee, F. S.; Hagler, J.; Chen, Z. J.; Maniatis, T. Activation of the IkappaB alpha kinase complex by MEKK1, a kinase of the JNK pathway. *Cell* **1997**, *88*, 213–222.
(29) Jarrard, D. F.; Blitz, B. F.; Smith, R. C.; Patai, B. L.; Rukstalis, D.B. Effect of epidermal growth factor on prostate cancer cell line PC3 growth and invasion. *Prostate* **1994**, *24*, 46–53.
(30) Seth, D.; Shaw, K.; Jazayeri, J.; Leedman, P. J. Complex post-transcriptional regulation of EGF-receptor expression by EGF and TGF-alpha in human prostate cancer cells. *Br. J. Cancer* **1999**, *80*, 657–669.

Received for review December 1, 2008. Revised manuscript received January 23, 2009. Accepted February 13, 2009. This study was supported in part by grants from the National Science Council (NSC95-2320-B-039-044-MY2), and the China Medical University (CMU95-313, CMU96-115 and CMU96-212).

JF803725H